

Meta Clustering Learning for Large-scale Unsupervised Person Re-identification

Xin Jin*

jinxin@eias.ac.cn
Eastern Institute for Advanced Study

Tianyu He

deeptimhe@gmail.com
Alibaba Group

Xu Shen

shenxu.sx@alibaba-inc.com
Alibaba Group

Tongliang Liu

tongliang.liu@sydney.edu.au
The University of Sydney

Xinchao Wang

xinchao@nus.edu.sg
National University of Singapore

Jianqiang Huang

jianqiang.jqh@gmail.com
Alibaba Group

Zhibo Chen

chenzhibo@ustc.edu.cn
University of Science and Technology
of China

Xian-Sheng Hua

huaxiansheng@gmail.com
Alibaba Group

ABSTRACT

Unsupervised Person Re-identification (U-ReID) with pseudo labeling recently reaches a competitive performance compared to fully-supervised ReID methods based on modern clustering algorithms. However, such clustering-based scheme becomes computationally prohibitive for large-scale datasets, making it infeasible to be applied in real-world application. How to efficiently leverage endless unlabeled data with limited computing resources for better U-ReID is under-explored. In this paper, we make the first attempt to the large-scale U-ReID and propose a “small data for big task” paradigm dubbed Meta Clustering Learning (MCL). MCL only pseudo-labels a subset of the entire unlabeled data via clustering to save computing for the first-phase training. After that, the learned cluster centroids, termed as meta-prototypes in our MCL, are regarded as a proxy annotator to softly annotate the rest unlabeled data for further polishing the model. To alleviate the potential noisy labeling issue in the polishment phase, we enforce two well-designed loss constraints to promise intra-identity consistency and inter-identity strong correlation. For multiple widely-used U-ReID benchmarks, our method significantly saves computational cost while achieving a comparable or even better performance compared to prior works.

CCS CONCEPTS

• Information systems → Top-k retrieval in databases.

KEYWORDS

Clustering, Unsupervised Person Re-identification, Computational Cost Saving

*Corresponding Author.

Permission to make digital or hard copies of all or part of this work for personal or classroom use is granted without fee provided that copies are not made or distributed for profit or commercial advantage and that copies bear this notice and the full citation on the first page. Copyrights for components of this work owned by others than ACM must be honored. Abstracting with credit is permitted. To copy otherwise, or republish, to post on servers or to redistribute to lists, requires prior specific permission and/or a fee. Request permissions from permissions@acm.org.

MM '22, October 10–14, 2022, Lisboa, Portugal

© 2022 Association for Computing Machinery.

ACM ISBN 978-1-4503-9203-7/22/10...\$15.00

<https://doi.org/10.1145/3503161.3547900>

ACM Reference Format:

Xin Jin, Tianyu He, Xu Shen, Tongliang Liu, Xinchao Wang, Jianqiang Huang, Zhibo Chen, and Xian-Sheng Hua. 2022. Meta Clustering Learning for Large-scale Unsupervised Person Re-identification. In *Proceedings of the 30th ACM International Conference on Multimedia (MM '22)*, October 10–14, 2022, Lisboa, Portugal. ACM, New York, NY, USA, 11 pages. <https://doi.org/10.1145/3503161.3547900>

1 INTRODUCTION

Ubiquitous cameras generate innumerable pedestrian data every day. Due to the growing demands on person re-identification (ReID) and its expensive labeling cost, unsupervised person ReID (U-ReID) [9, 12, 14, 22, 30, 31, 33, 40, 49, 63, 65, 67, 78] has attracted increasing attention recently.

There are mainly two categories in U-ReID. One is unsupervised domain adaptive (UDA) person ReID, which first pre-trains a model on the labeled source dataset, and then fine-tunes the model on the unlabeled target dataset to reduce domain gap [11, 35, 55, 58, 65, 75, 76]. Albeit effective, UDA ReID branch typically suffers from a complex adaptation process, and its success also relies on an assumption that the discrepancy between source and target domain is not significant. This motivates the exploration on the other branch, the clustering-based unsupervised ReID [9, 14, 18, 22, 36, 54]. As the “Previous work” shown in Figure 1, the works of this branch tend to perform an iterative optimization process of *feature extraction–clustering–train*. In this way, all unlabeled data can be explicitly leveraged with the pseudo labels generated by clustering. The focus of the recent clustering-based methods lies in creating more reliable clusters and efficiently using them to learn discriminative representations, e.g., with the help of self-similarity grouping [18], hybrid memory bank with contrastive loss [22] or cluster-level memory bank [9], multi-label classification [54], and online hierarchical cluster dynamics [66, 71].

However, these methods all neglect an important fact in practice: the clustering process costs an intolerable computational resources due to its pair-wise similarity calculation and neighboring samples searching. Taking the most common clustering algorithm DBScan [13] in U-ReID as example, its worst time complexity and space complexity are both $O(n^2)$. When the size of unlabeled data is very large (as shown in Figure 1(a)), both of the memory and time

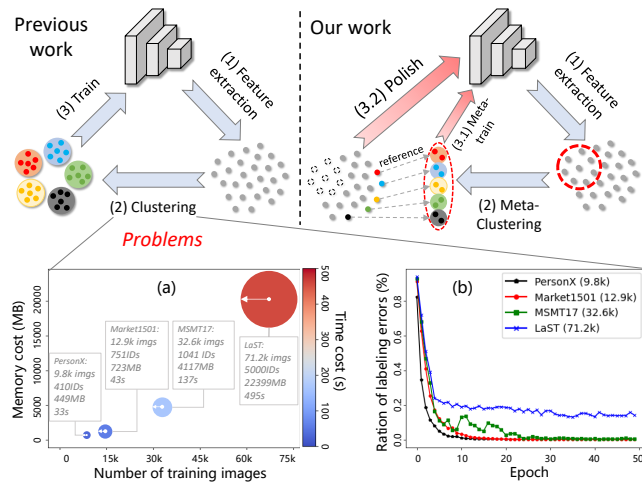


Figure 1: Motivation illustration for clustering-based unsupervised ReID: as the size of unlabeled data increases, the clustering process in previous works will (a) cost an intolerable computational resources in terms of memory and time costs, and (b) be more prone to be affected by pseudo label noise. Our work introduces a new meta-clustering learning to achieve a satisfactory U-ReID performance while simultaneously tackling these two challenges.

cost of clustering will rapidly increase. For example, performing clustering once on the LaST [45] (71.2k images) on the GPU following previous works [9, 22, 30] will take a memory usage up to 22GB, which can not run on a 16GB Tesla V100. One may ask why not use the offline clustering (on CPU) or batch-wise local clustering (e.g., K-means) to avoid a large memory and time cost. This is due to the specificity of ReID: (1) the clustering-based ReID needs iteratively perform the feature extraction and clustering **in feature domain** (on GPU) [9, 22, 54]; (2) the batch-wise local clustering for ReID is sub-optimal, which hinders the exploration and utilization of global relationship among large-scale person data.

In this paper, we attempt to achieve a large-scale unsupervised ReID framework while taking the computational cost into account, which is challenging but valuable and meaningful to bridge the gap between ReID algorithms and practical applications. To this end, we propose a “small data for big task” paradigm dubbed Meta Clustering Learning (MCL). Inspired by the other concept of Meta Learning [51–53] that are designed for ‘learning to learn’ with the assistance of meta knowledge, our MCL first obtain the meta knowledge on a part of the unlabeled person data and then softly extend the knowledge to the rest unlabeled ones. Therefore, it naturally avoids clustering the full/whole dataset before each training epoch and thus reduces the computation overhead. In addition, during the knowledge extension process, MCL further leverages a clustering-free polishing step to enhance the discriminative representation learning while alleviating noisy label issue for ReID model.

As illustrated in Figure 1, MCL consists of two phases of meta-prototype optimization and prototype-referenced polishment (see Sec. 3.1, 3.2 for details). In the first phase, the features of the *partial*

unlabeled images are extracted. This ratio can be flexibly determined according to the computing power of practical environment, as a by-product of MCL. Then, a clustering algorithm, like DB-Scan [13], is used to cluster features and generate pseudo ID labels. Based on them, the ReID model is trained with a memory-based optimization strategy [9, 22, 54]. Meanwhile, the clustered centroids (termed as meta-prototypes) are stored in the memory and updated on the fly in a momentum manner [24].

The second prototype-referenced polishment is based on the learned meta-prototypes in the previous phase, which are taken as a proxy annotator to mine the potential label information for *the rest unlabeled data*. For each unused person image, we get a soft real-valued label likelihood vector by comparing it with meta-prototypes reference. Based on such clustering-free pseudo label, we further polish model by mining the relative comparative characteristic in person images. The reason why we call this phase as “polishment” is because “polish” has the meaning of try to perfect one’s skill, like here we promote the discriminative feature learning for ReID model with *the rest unlabeled data*.

Another point should be noticed is that, the pseudo labeling itself no matter of clustering-based or reference-based may generate wrong label predictions [20, 30, 54, 60]. As shown in Figure 1(b), the larger size of unlabeled dataset, the more possible of generating noisy labels. To alleviate it, we further leverage two loss constraints for label denoising in MCL. One loss enforces instance-level consistency to reduce intra-identity variance and the other constructs a soft-weighted triplet constraint to promise inter-identity correlation. In this way, MCL could better investigate the discriminative information of data even with noisy pseudo labels. We summarize our main contributions as follows:

- To our best knowledge, this paper is the first to achieve the unsupervised large-scale ReID training while considering the computational cost savings. A “small data for big task” paradigm dubbed Meta Clustering Learning (MCL) is proposed. MCL performs clustering-based ReID training on **partial** unlabeled data, saving computing resources.
- To further leverage the rest unlabeled data, we take the learned prototypes from **partial** data as proxy annotator to pseudo-label them, and then polish model based on such pseudo labels with two well-designed losses (as a minor contribution) to promise intra-identity consistency and inter-identity strong correlation, which helps alleviate the noisy label issue.
- As the first attempt to handle the large-scale unsupervised ReID, extensive experiments on multiple benchmarks show that MCL could significantly save computational cost while achieving a state-of-the-art performance. In particular, MCL achieves ReID performance improvements of 4.8%, 2.9% in mAP on the large-scale MSMT17 [58], LaST [45], but saves 71.8%/87.9% memory costs and 73.7%/85.7% time costs compared to the baselines.

2 RELATED WORK

2.1 Unsupervised Person Re-identification

Unsupervised Domain Adaptive (UDA) ReID. This branch usually utilizes transfer learning, e.g., style translation [77], to reduce domain gap between source and target ReID scenarios for adaptation [8, 11, 38, 58, 69]. Their performance is typically inferior to the

clustering-based approaches, since there is still a gap between the style-translated images and the realistic person images [56, 62].

Clustering-based Unsupervised ReID. This branch typically trains ReID model directly on unlabeled dataset with a clustering-based pseudo label estimation [14, 18, 46, 62, 63, 68, 72]. This clustering labeling and training process are usually alternatively performed until the model is stable. In particular, Lin *et al.* [36] treat each individual sample as a cluster, and then gradually group similar samples into one cluster to generate pseudo labels. Jin *et al.* [30] introduce a global distance-distribution separation constraint to handle the sample-wise noisy label. SPCL [22] proposes a self-paced contrastive learning framework to gradually create more reliable clusters for ReID training while updating the hybrid memory containing both source and target domain features. Similarly, ClusterContrast [9] further stores feature vectors inside a cluster-level memory to alleviate the inconsistent clustering issue. Recently, Isobe *et al.* [28] introduce cluster-wise contrastive learning (CCL), progressive domain adaptation (PDA), Fourier augmentation (FA), and ICE [3] introduces inter-instance contrastive encoding to boost the existing class-level contrastive ReID methods. However, all these methods focus on how to get more reliable pseudo labels or how to better leverage them for discriminative feature learning, an important point of computational cost is still under-explored. Besides, the noisy pseudo label issue in these methods has not yet been well addressed.

Reference-based Pseudo Labeling in ReID. Existing representative works, like MAR [65], MMCL [54], MPRD [29], and SSL [37] either use labeled source data for pseudo labels generation or assign each unlabeled person image with a multi-class/softened label via pairwise similarity computation. Differently, our MCL creates clustering-free soft pseudo labels with the reference of online updated meta-prototypes that stored in the memory. Such design is more efficient because it does not need source labeled dataset as reference, and meta-prototypes (like a FC layer) could help directly infer out real-valued labels instead of repeat pairwise comparisons. Moreover, more reliable meta-prototypes encourage more accurate pseudo labeling (more effective unsupervised training), and vice versa. They promote each other, achieving a win-win effect.

2.2 Self-supervised Representation Learning

MCL is also related to self-supervised representation learning (SSL). Based on contrastive learning framework, SSL has achieved a great success [15, 41], *e.g.*, MoCo [24], MoCov2 [6], SimCLR[4], SimCLRv2 [5], BYOL [23], and SimSiam [7]. Their main idea is to match a same instance in different augmented views, which typically relies on a large number of explicit pairwise feature comparisons and faces a computational challenge. Besides, these **instance-wise** SSL methods can not directly address the **fine-grained** unsupervised ReID problem (they can only be taken for pre-training/initialization [16, 17, 64]), because ReID needs the cluster priors to mine fine discriminative clues.

3 META CLUSTERING LEARNING (MCL)

Overview. To tackle the computing challenge in large-scale U-ReID, we propose a meta clustering learning (MCL), which is a unified episodic training framework, and comprises two phases of

meta-prototype optimization (Figure 2) and prototype-referenced polishment (Figure 3). MCL alternates between these two phases: (1) group the *partial* unlabeled data into clusters and store the learned meta-prototypes, while training model with cluster-level contrastive loss (Section 3.1); (2) use meta-prototypes as reference to annotate the *rest* unlabeled samples for further fine-tune, and two loss constraints are enforced to promise intra-identity consistency and inter-identity correlation (Section 3.2).

Given an unlabeled dataset \mathbb{X} , MCL first splits \mathbb{X} into N subsets uniformly, and then randomly selects one as *meta-training subset* \mathbb{X}_1 for meta-prototype optimization, *the rest subsets* $\mathbb{X}_2, \mathbb{X}_3, \dots, \mathbb{X}_N$ are taken for prototype-referenced polishment. This split is performed before each training epoch.

3.1 Phase 1: Meta-prototype Optimization

MCL costs less resources in clustering by only using a meta-training subset \mathbb{X}_1 .

Feature Extraction and Clustering. As shown in Figure 2, a network f_θ (*e.g.*, ResNet-50 [25], initialized with pre-trained weights on ImageNet [9, 21, 22, 28]) is taken as backbone to extract features from \mathbb{X}_1 . Then, DBScan [13] is used to cluster these features (unclustered outliers are discarded [3, 9]). The *IDs* of cluster results are assigned to unlabeled samples as the pseudo labels for training.

Query Setup and Meta-prototype Initialization. After obtaining clustered pseudo labels for \mathbb{X}_1 , we sample P person identities and I instances for each identity, to set up a mini batch with the size of $P \times I$. Different from works [30, 46] that directly use the instance-wise loss constraints (*e.g.*, triplet loss [27]) for training, we take each batch as a query set and employ a memory dictionary based contrastive learning [9, 22, 28] for optimization.

We maintain a group of learnable meta-prototypes $\{\mathbf{w}_1, \dots, \mathbf{w}_K\}$ stored in the memory dictionary. Here, K is same with the number of clustered clusters, which is always changing during the training. Particularly, the clustering algorithm (*e.g.*, DBScan) is performed before each training epoch, and then the **epoch-wise** meta-prototypes are initialized with the mean feature vectors of each cluster, *i.e.*, $\mathbf{w}_k = \frac{1}{|\mathbb{I}_k|} \sum \mathbf{v}_i$, where \mathbf{v}_i means i -th feature vector of k -th cluster, \mathbb{I}_k denotes the k -th set that contains all the feature vectors within cluster k , and $|\cdot|$ denotes the number of features in the set.

Meta-prototypes Update and Model Optimization. At each iteration t of epoch, the encoded feature vectors $\{q\}$ of $P \times I$ query images in each mini-batch would be involved in meta-prototypes update. With the momentum updating [24], the k -th cluster prototype \mathbf{w}_k is updated by the mean of encoded query features belonging to class k ,

$$\mathbf{w}_k^t \leftarrow m \cdot \mathbf{w}_k^{t-1} + (1 - m) \cdot \frac{1}{|\mathbb{B}_k^t|} \sum_{q_i^t \in \mathbb{B}_k^t} q_i^t, \quad (1)$$

where \mathbb{B}_k^t denotes the feature vector set belonging to class k in the mini-batch at the t -th iteration, and $m \in [0, 1]$ is a momentum coefficient, which is empirically set as 0.2 following [9, 22]. The learned meta-prototypes are taken for model optimization together with query samples in this phase, and also play a role of proxy annotator (see the ‘robot’ in Figure 2,3) for the rest unlabeled subsets $\mathbb{X}_2, \mathbb{X}_3, \dots, \mathbb{X}_N$ in the next phase.

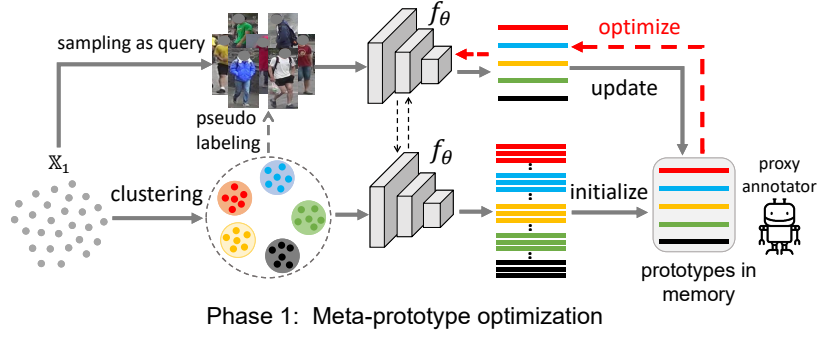


Figure 2: The first training phase in one training epoch of MCL. Features of *partial* data (meta-training subset \mathbb{X}_1) are assigned pseudo labels by clustering, and the same color represents the same class. The lower part is the memory initialization while the upper part is the model training. A contrastive loss is calculated for optimization between query features and all prototypes in memory.

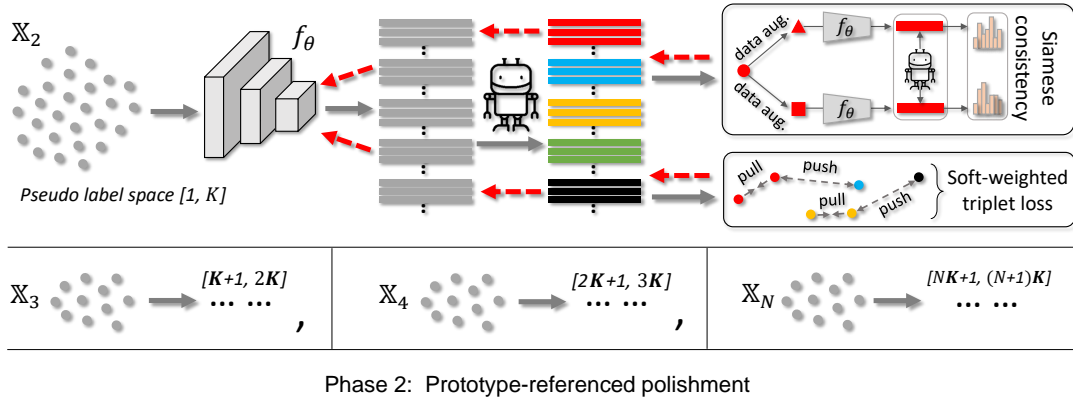


Figure 3: The second phase in one training epoch of MCL. The rest unlabeled subsets $\mathbb{X}_2, \mathbb{X}_3, \dots, \mathbb{X}_N$ are assigned soft pseudo labels by comparing with the learned meta-prototypes (*i.e.*, the proxy annotator of ‘robot’) for ReID model polishment. Siamese consistency loss \mathcal{L}_{sc} and soft-weighted triplet loss \mathcal{L}_{tri}^{sw} are enforced to alleviate the noisy pseudo label issue. Note that, this clustering-free polishment is performed on all subsets $\mathbb{X}_2, \mathbb{X}_3, \dots, \mathbb{X}_N$ together by cross-set sampling, with the non-overlapping label space.

With respect to the loss function in the first phase, we use a general contrastive loss [9, 22] for model optimization. Basically, given a query instance q , we compare it to all meta-prototypes $\{\mathbf{w}_1, \dots, \mathbf{w}_K\}$ using InfoNCE loss [39]:

$$\mathcal{L}_{phase1} = -\log \frac{\exp(\mathbf{q} \cdot \mathbf{w}^+ / \tau)}{\sum_{i=0}^K \exp(\mathbf{q} \cdot \mathbf{w}_i / \tau)} \quad (2)$$

where \mathbf{w}^+ is the positive cluster prototype vector to query instance q and τ is a temperature hyper-parameter per [61].

3.2 Phase 2: Prototype-referenced Polishment

To achieve the savings of clustering cost, the first meta-prototype optimization phase only uses a part of unlabeled data, *i.e.*, the meta-training subset \mathbb{X}_1 . The rest unlabeled subsets $\mathbb{X}_2, \mathbb{X}_3, \dots, \mathbb{X}_N$ are leveraged in a clustering-free manner in this second phase. Basically, we take the learned meta-prototypes $\{\mathbf{w}_1, \dots, \mathbf{w}_K\}$ from the first phase as proxy annotator to softly mine discriminative information for those rest unlabeled data for model polishment. This two-phase

training is equivalent to traverse the entire dataset once, *i.e.*, one epoch.

Prototype-referenced Labeling. For clarity, we take an unused and unlabeled subset \mathbb{X}_2 as example for illustration. Given $\mathbb{X}_2 = \{x_i\}_{i=0}^{N_2}$ where each x_i is a collected unlabeled person image, the learned meta-prototypes $\{\mathbf{w}_1, \dots, \mathbf{w}_K\}$ defines the pseudo label space for \mathbb{X}_2 is $[1, K]$. As shown in the ‘robot’ in Figure 3, the meta-prototypes set $\{\mathbf{w}_k\}_{k=1}^K$ is taken as proxy annotator, a soft real-valued pseudo label \mathbf{y}_i can be assigned for x_i by comparing $f(x_i)$ with the reference agents $\{\mathbf{w}_k\}_{k=1}^K$. This soft prototype-referenced pseudo labeling process is,

$$y_i^j = L(f(x_i), \{\mathbf{w}_k\}_{k=1}^K)^j = \frac{\exp(\mathbf{w}_j^T f(x_i))}{\sum_k \exp(\mathbf{w}_k^T f(x_i))}, \quad (3)$$

where $L(\cdot)$ means a soft pseudo labeling function. This function is epoch-wise and acts like a dimension-variable FC layer (*i.e.*, dot-product). $y_i^j \in (0, 1)$ is the j -th entry of \mathbf{y}_i . All dimensions of \mathbf{y}_i add up to 1 and each dimension represents the label likelihood

w.r.t. a reference prototype person ID. Different from the vanilla reference-based pseudo labeling [65] or using a global classifier for labeling, our prototype-referenced labeling allows the **epoch-wise** and **dimension-variable** proxy annotator $\{\mathbf{w}_k\}_{k=1}^K$ to be updated on the fly. More reliable meta-prototypes encourage more accurate labeling and thus more effective optimization, and vice versa. Besides, the clustering results are different (K is changing) for each epoch in ReID, an immutable global classifier is infeasible.

Last but not least, as shown in Figure 3, the label spaces for different subsets $\mathbb{X}_2, \mathbb{X}_3, \dots, \mathbb{X}_N$ are manually designed as non-overlapping by considering two aspects: 1) the learned meta-prototypes $\{\mathbf{w}_k\}_{k=1}^K$ can only cover a limited number of person identities (K IDs) of the entire dataset, especially when the meta-training subset \mathbb{X}_1 is very small. 2) assigning different subsets with different label spaces could increase the identity diversity, which simulates the real scenario where each person has multiple images from different views (see Sec. 4.4 in experiment).

Polish the Model with Soft Pseudo Labels. An intuitive solution is to ‘harden’ the obtained soft pseudo labels, *i.e.*, regard the dimension with the largest value as person ID, *i.e.*, $J = \arg \max \{y^j\}_{j=1}^K$. Based on these identity labels J s, we can construct ReID constraints for training, such as cross-entropy loss [19, 48] and triplet loss [27]. In fact, our early attempts along this line have failed to deliver very good results. We analyze that is because the reference-based pseudo labeling itself will inevitably introduce some noisy labels. To exploit the merits of the prototype-referenced labeling while alleviating the noisy label effect, we additionally introduce two well-designed loss constraints to better leverage these *unsatisfactory* soft pseudo labels for optimization, by considering the intra-identity consistency between different views within each person identity and the inter-identity correlations among different persons. They are shown in the two black boxes in Figure 3 and elaborated below: **Siamese consistency Loss** \mathcal{L}_{sc} is the first constraint to promise consistency within the same identity. As shown in the upper black box in Figure 3, \mathcal{L}_{sc} is built on the “swapped” prediction idea of SwAV [2] to predict the label of a view from the representation of another view. Given two features \mathbf{f}_s and \mathbf{f}_t extracted from two different augmentations of *the same image*, we compute their referenced pseudo labels \mathbf{y}_s and \mathbf{y}_t following Eq.(3) by matching these features to the learned meta-prototypes $\{\mathbf{w}_k\}_{k=1}^K$:

$$\begin{aligned} \mathcal{L}_{sc}(\mathbf{f}_s, \mathbf{f}_t) &= \mathcal{L}_{ce}(\mathbf{f}_s, \mathbf{y}_t) + \mathcal{L}_{ce}(\mathbf{f}_t, \mathbf{y}_s) \\ \mathcal{L}_{ce}(\mathbf{f}_s, \mathbf{y}_t) &= - \sum_k \mathbf{y}_t^{(j)} \log \mathbf{p}_s^{(j)}, \quad \text{where } \mathbf{p}_s^{(j)} = \frac{\exp(\mathbf{w}_j^\top \mathbf{f}_s)}{\sum_k \exp(\mathbf{w}_k^\top \mathbf{f}_s)}, \end{aligned} \quad (4)$$

where $\mathcal{L}_{ce}(\mathbf{f}_s, \mathbf{y}_t)$ measures the fit between features \mathbf{f}_s and soft pseudo label \mathbf{y}_t . Intuitively, if these two features capture the same person information, they should be able to predict from each other. \mathcal{L}_{ce} is the cross entropy loss between the label and the probability obtained by taking a softmax of the dot products of \mathbf{f} and all prototypes in $\{\mathbf{w}_k\}_{k=1}^K$.

Soft-weighted Triplet Loss \mathcal{L}_{tri}^{sw} is the second constraint which softly leverages the *relative* correlations between identities to construct weighted-triplets for optimization. Considering the soft pseudo labels are continuous real-valued, a soft-weighted triplet loss \mathcal{L}_{tri}^{sw}

is enforced to promise the correct *relative* correlation among person identities. Let $\{x^a, x^p, x^n\}$ be an input triplet sample and the corresponding feature embeddings are $\{f(x^a), f(x^p), f(x^n)\}$, the soft-weighted triplet loss is given by,

$$\begin{aligned} \mathcal{L}_{tri}^{sw} &= \omega(a, p, n) [\|f(x^a) - f(x^p)\|_2^2 - \|f(x^a) - f(x^n)\|_2^2 + m]_+, \\ \omega(a, p, n) &= \langle f(x^a), f(x^p) \rangle \langle f(x^a), f(x^n) \rangle \end{aligned} \quad (5)$$

where $\omega(a, p, n)$ and m are the loss weighting factor and margin factor (0.3 by fault), $\langle \cdot \rangle$ means the similarities between feature vectors, which adaptively alters the magnitude of the triplet loss in a soft manner. In general, when the anchor-positive pair is similar (*i.e.*, $\langle f(x^a), f(x^p) \rangle$ is high), the sample is more confident and reliable. Likewise, when the anchor-negative pair is similar (*i.e.*, $\langle f(x^a), f(x^n) \rangle$ is high), it forms a *hard negative example* [44]. Hence, \mathcal{L}_{tri}^{sw} can give a higher priority and more attention on these reliable and hard cases, so as to alleviate the noisy label issue.

4 EXPERIMENT

4.1 Datasets and Implementation

Datasets and Evaluation. We evaluate the proposed MCL method on multiple ReID benchmarks (from small to large scale): PersonX (PX) [47], Market1501 (Ma) [70], MSMT17 (MT) [58], and the largest public ReID dataset (so far) LaST (LS) [45]. To further show the superiority of MCL in the large-scale data setting, we also conduct experiments on the *mixed* datasets, *e.g.*, training on multiple datasets $PX+Ma+MT+LS$ while testing on unseen test set of *MT*. The details about datasets are shown in Table 1.

Implementation Details. The proposed MCL is generic and can be applied to different clustering-based U-ReID backbones. Here, we re-implement ClusterContrast [9] as baseline, since it has been dominating the leaderboard in multiple benchmarks w.r.t unsupervised ReID performance, and is considerably more efficient as a source-free purely unsupervised ReID pipeline compared to those competitive adaptive (source data needed) U-ReID algorithms, like MMT [21], SpCL [22], [71] *etc.* ResNet-50 [25] is adopted as the backbone of the feature extractor and initialize the model with the parameters pre-trained on ImageNet [10].

At the beginning of MCL training, we first train the ReID model only with the first phase of *meta-prototype optimization* (skip the second phase of *prototype-referenced polishment*), which aims to warm up the *meta-prototype* learning, like the FC layer warm-up [25, 43], so as to have a reasonable pseudo labeling for the next model polishing. This process lasted for 5 epochs for PersonX, and 10epochs for Market1501, MSMT17, and LaST. For image size, the input is resized as 256×128 (height×width) for all person datasets. For data augmentation, we perform random horizontal flipping, padding with 10 pixels, random cropping, and random erasing [74]. For batch size, each mini-batch contains 256 images of 16 pseudo person identities

Table 1: Introduction and comparison of datasets we used.

Dataset	Style	Train IDs	Train images	Test IDs	Query images	Total images	Cameras
PersonX [47]	Synthetic	410	9,840	856	5,136	45,792	6
Market-1501 [70]	Real	751	12,936	750	3,368	32,668	6
MSMT17 [58]	Real	1,041	32,621	3,060	11,659	126,441	15
LaST [45]	Real	5,000	70,923	5,803	10,173	228,156	*

Table 2: Memory&Time Cost vs. Unsupervised ReID Performance (%). In which, $M(MB)$, $T(s)$ denotes the *memory cost*, *time cost* of performing clustering once in training, where ‘s’ means ‘second’. $T(h)$ denotes the total training time where ‘h’ means ‘hour’. We compare several MCL variants to baseline (*All*, i.e., Full Clustering scheme) by using 50%, 33%, 25%, and 20% data randomly selected from the entire unlabeled dataset as meta-training subset \mathbb{X}_1 . For the smallest dataset PersonX [47], it is not necessary to do experiments with too harsh computational requirements (e.g., 33%, 25%, 20%). We can see that the larger size of unlabeled dataset, the more superior of our method (red). Note that, the DukeMTMC-ReID dataset [42] has been taken down and thus not used in our experiment, we just use PersonX [47], Market1501 [70], MSMT17 [58], and LaST [45] for experiments.

Methods	PersonX (9.8k imgs, 410 IDs)					Market1501 (12.9k imgs, 751 IDs)					MSMT17 (32.6k imgs, 1041 IDs)					LaST (71.2k imgs, 5000 IDs)				
	mAP	Rank1	M (MB)	T (s)	T (h)	mAP	Rank1	M (MB)	T (s)	T (h)	mAP	Rank1	M (MB)	T (s)	T (h)	mAP	Rank1	M (MB)	T (s)	T (h)
All	88.5	95.8	822.3	30.0	2.7	83.3	93.0	876.3	34.3	2.9	33.4	62.9	6251.5	118.3	9.3	19.8	74.0	22398.5	494.8	42.0
50%	79.0	93.5	412.6	13.1	2.2	82.9	92.7	348.6	10.8	2.4	38.2	66.5	1761.3	31.1	4.6	20.0	74.9	5779.6	121.2	20.0
33%	-	-	-	-	-	79.6	91.9	287.5	7.0	2.2	31.5	57.4	889.1	18.2	3.8	22.7	75.0	2688.2	70.8	14.0
25%	-	-	-	-	-	75.4	89.3	235.1	5.4	2.0	25.9	53.4	556.9	13.4	3.0	17.2	69.0	1564.2	44.7	9.0
20%	-	-	-	-	-	41.3	61.3	141.4	4.6	1.9	20.1	47.4	394.6	10.3	2.6	15.8	56.0	1066.0	38.4	7.0

(16 instances for each person). During the training, we adopt Adam optimizer to train the ReID model with weight decay $5e-4$. The initial learning rate is set to $3.5e-4$, and is decayed by a factor of 0.1 every 20 epoch in a total of 60 epoch. Following [9, 22], we use DBScan and Jaccard distance [73] to cluster with k nearest neighbors, where $k=30$. For DBScan, the maximum distance d between two samples is experimentally set as 0.4 for market1501, 0.7 for other datasets, and the minimal number of neighbors in a core point is all set as 4.

4.2 Effectiveness and Necessity of MCL

Memory&Time Cost vs. U-ReID Performance. Table 7 shows the U-ReID performance resulted by using subsets of size 50%, 33%, 25%, and 20% randomly selected from all unlabeled data as meta-training set \mathbb{X}_1 vs. directly conducting clustering over full data (*All*). We observe that using *partial* data for clustering with MCL effectively saves computational costs on both memory and time. For example, the *MCL*, 50% schemes nearly achieve the same ReID performance but save memory&time cost by over 50%, such savings are particularly obvious on the large datasets: 1761.3MB, 31.1s vs 6251.5MB, 118.3s on MSMT17 and 5779.6MB, 121.2s vs 22398.5MB, 494.8s on LaST. However, we also observe that the ReID performance of mAP/Rank1 has a noticeable drop, especially on the small dataset PersonX (‘blue’ in Table 7). We analyze that’s because the noisy label issue will be enlarged on small datasets.

Interestingly, in contrast to the trend in Memory&Time saving vs. ReID accuracy reduction, we find an opposite trend for mAP/Rank1 improvements on the two largest datasets MSMT17 and LaST (‘red’ in Table 7). This reveals that the larger of unlabeled dataset, the more superior of our method. We analyze such gains come from two aspects: 1). less meta-training data gets more reliable clustered results; 2). the prototype-referenced polishment with intra- and inter-identity constraints promotes the discriminative ReID feature learning.

Necessity of MCL. Someone may think of directly splitting a large-scale dataset into multiple small subsets to do clustering-based U-ReID sequentially. This is also the most straightforward solution to handle the computational issue we focused. To study its feasibility, we deliberately design a scheme named *Naive Splitting*

Table 3: Study on the necessity of our MCL. For the scheme of *Naive Splitting Training*, several subsets picked from one single large data set are *sequentially* used for *clustering*→*labeling*→*training* (same with phase-1 in MCL).

Methods	Market1501		MSMT17		
	mAP	Rank1	mAP	Rank1	
50%	Naive Splitting Training	73.6	82.2	22.2	43.9
	MCL	82.9 (↑9.3)	92.7 (↑10.5)	38.2 (↑16.0)	66.5 (↑22.6)
25%	Naive Splitting Training	68.4	74.1	16.2	36.5
	MCL	75.4 (↑7.0)	89.3 (↑15.2)	25.9 (↑9.7)	53.4 (↑16.9)

Training, where multiple subsets picked from one single large data set are *sequentially* used for *clustering*→*labeling*→*training*. *Naive Splitting Training* also could save memory cost due to its subset-wise clustering, but this operation also inadvertently enlarges the negative effect of time consuming and noisy labeling. As shown in Table 3, two *Naive Splitting Training* schemes of using 50%/25% subset as training unit, are inferior to *MCL* by 16.0%/9.7% in mAP on MSMT17, which reveals two facts that 1) naively splitting the holistic large-scale dataset for sequential training is not optimal, and 2) *MCL* is necessary and more superior.

4.3 Study on Mixed Large-scale Datasets

As discussed in Sec. 4.2 and Table 7, the larger size of unlabeled dataset, the more superior of MCL. To fully study this point, we further construct two *mixed* large-scale training datasets $PX+Ma+MT$ and $PX+Ma+MT+LS$, and evaluate models on the unseen test set of MSMT17 (*MT*). Note that, we originally planned to perform such group of experiments on the larger realistic ReID datasets, but which is limited by the truth that most large-scale realistic ReID datasets (e.g., Person30K [1], FastHuman [26]) have not fully released. As shown in Table 4, we can get two observations: 1). the scheme of *All* on the largest dataset $PX+Ma+MT+LS$ is failed to be directly clustered/trained due to the computing pressure. 2). *MCL* outperforms *All* by 2.3% in mAP under 50% on $PX+Ma+MT$ → MT 3). *MCL* performs better on $PX+Ma+MT$ than that on $PX+Ma+MT+LS$,

Table 4: Study on mixed large-scale datasets, where PX , Ma , MT , LS denotes *PersonX*, *Market1501*, *MSMT17*, *LaST*. Note that, in the experimental environment with four 16GB Tesla V100 GPUs, the scheme of *All* on $PX+Ma+MT+LS$ is failed to be directly clustered/trained due to the computing pressure.

Train Datasets	Methods	Test: MT			
		mAP	Rank1	M (MB)	T (s)
MT	All	33.4	62.9	6251.5	118.3
PX+Ma+MT	All	29.6	56.3	29788.7	244.8
	MCL, 50%	31.9	59.3	7698.3	82.6
	MCL, 25%	23.1	49.6	1399.0	35.9
PX+Ma+MT+LS	All	–	–	–	–
	MCL, 50%	25.5	49.9	21207.8	323.3
	MCL, 25%	17.1	39.5	5126.9	107.5

which may be due to the style/domain gap between LaST [45] and other ReID datasets.

4.4 Ablation Study

Influence of Loss Constraints. We study the effectiveness of the proposed siamese consistency loss \mathcal{L}_{sc} and soft-weighted triplet loss \mathcal{L}_{tri}^{sw} in Table 5a. We see that *MCL* outperforms *MCL w/o \mathcal{L}_{sc}* by **4.0%/3.2%** in mAP for 50%/25% settings on Market1501. When replace the soft-weighted triplet loss \mathcal{L}_{tri}^{sw} with the basic triplet loss version [27], the scheme of *MCL w/o \mathcal{L}_{tri}^{sw}* is inferior to *MCL* by **5.6%/4.4%** in mAP for 50%/25% settings on Market1501. Such two constraints facilitate the pseudo label denoising via promising intra-identity consistency and inter-identity correlation. In addition, they are complementary and both vital to MCL, jointly resulting in a superior performance.

Influence of Data Split. As we described before Sec. 3.1, given an unlabeled dataset \mathbb{X} , we use a random and uniform split strategy to divide the samples into *meta training subset* \mathbb{X}_1 and *the rest subsets* $\{\mathbb{X}_2, \mathbb{X}_3, \dots, \mathbb{X}_N\}$. Such split is performed before each training epoch. And, the label spaces for different subsets $\{\mathbb{X}_1, \mathbb{X}_2, \mathbb{X}_3, \dots, \mathbb{X}_N\}$ are same-size but non-overlapping. Here we study on the influence of different split designs. In Table 5b, the scheme of *MCL_fixed* means we only conduct the data split once at beginning and fix the split results during the training. *MCL_same* means the scheme where all subsets share the same label space. We can observe that *MCL_fixed* is inferior to *MCL* by 11.4%/37.6% in mAP under 50%/25% on Market1501, and *MCL_same* is inferior to *MCL* by 15.6%/11.5% in mAP under 25% on Market1501/MSMT17. We analyze that: 1). re-splitting dataset before each epoch plays a role of data re-organization, like the mechanism behind cross-validation [32], which avoids overfitting and extremely cases, increasing robustness of MCL. 2). non-overlapped label spaces increase the diversity of training data, like a data augmentation, promoting the discriminative ReID representations learning. Such design brings obvious improvements especially when using less meta-training data. For example, *MCL* outperforms *MCL_same* by only 2.1%/1.7% in mAP under 50%, but by 15.6%/11.5% under 25%. More analytic and ablated results (including limitation discussions) are presented in **Supplementary**.



Figure 4: Visual results of the same pseudo-labeled images on large-scale MSMT17 (two groups on the left) and LaST (two groups on the right), mined by using the general clustering technique and our meta-prototype referenced labeling. Green boxes denote correct results while red boxes denote false results. Important fine-grained feature clues are highlighted below each image pair. All faces in the images are masked for anonymization.

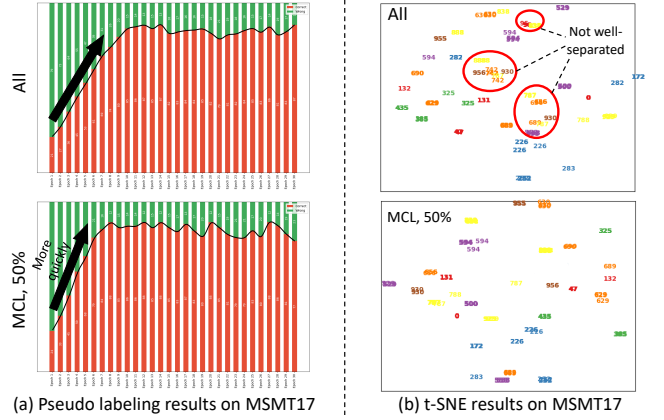


Figure 5: (a) Visualization of the percentages of correctly (red) and wrongly (green) pseudo labeling on MSMT17 as training goes on. (b) Visualization of t-SNE distributions on MSMT17. Different colors and digits represent different identities.

4.5 Visual Results and Insights

Visualization on Pseudo Labeling. To further show the proposed prototype-referenced labeling in MCL is superior to the general clustering, we compare these two pseudo-labeling methods by showing the same pseudo-labeled images (*i.e.*, the positive pairs) in Figure 4. Our scheme is *MCL, 50%*. We observe that: 1). for the general clustering, the grouped entries share the global visual similar appearance. This is not reliable enough. For example, in the most left pair of Figure 4, the two women are dressed very similarly, the only local discriminative clue is they take different items in their hands. 2). the proposed meta-prototype referenced labeling has the capability of discovering fine-grained discriminative clues (bottom in Figure 4) due to the usage of relative comparative characteristic among samples. This also explains why MCL outperforms the baseline scheme of *All* even with less data for clustering to some extent.

Moreover, we also count the proportions of correctly and wrongly clustering persons into the same category on MSMT17 in Figure 5 (a), we can see that *MCL, 50%* could achieve a better identity grouping performance more quickly compared to the baseline scheme of *All*.

Table 5: Ablation study for meta clustering learning (MCL).

(a) Study on the two loss constraints.					(b) Study on the data split strategies.						
Methods		Market1501		MSMT17		Methods		Market1501		MSMT17	
		mAP	Rank1	mAP	Rank1			mAP	Rank1	mAP	Rank1
50%	MCL w/o \mathcal{L}_{sc}	78.9	88.8	35.1	62.8	50%	MCL_fixed	71.5	87.8	21.2	44.0
	MCL w/o \mathcal{L}_{tri}^{sw}	77.3	86.4	33.4	60.7		MCL_same	80.8	92.0	36.5	63.8
	MCL	82.9	92.7	38.2	66.5		MCL	82.9	92.7	38.2	66.5
25%	MCL w/o \mathcal{L}_{sc}	72.2	84.8	20.4	44.5	25%	MCL_fixed	37.8	61.0	20.0	43.7
	MCL w/o \mathcal{L}_{tri}^{sw}	71.0	84.1	17.6	38.1		MCL_same	59.8	80.3	14.4	34.3
	MCL	75.4	89.3	25.9	53.4		MCL	75.4	89.3	25.9	53.4

Table 6: Comparison with state-of-the-art methods on the unsupervised ReID, including purely unsupervised methods and unsupervised domain adaptation (UDA) methods. “None” represents the former, and other value represents the source-domain dataset in UDA method.

(a) Experiments on Market1501.						(b) Experiments on MSMT17.					
Methods	Market1501					Methods	MSMT17				
	source	mAP	Rank1	Rank5	Rank10		source	mAP	Rank1	Rank5	Rank10
BUC [36]	None	38.3	66.2	79.6	84.5	TAUDL [33]	None	12.5	28.4	-	-
UGA [59]	None	70.3	87.2	-	-	MMCL [54]	None	11.2	35.4	44.8	49.8
SSL [37]	None	37.8	71.7	83.8	87.4	UTAL [34]	None	13.1	31.4	-	-
MMCL [54]	None	45.5	80.3	89.4	92.3	UGA [59]	None	21.7	49.5	-	-
HCT [66]	None	56.4	80.0	91.6	95.2	MMT [21]	Ma	24.0	50.1	63.5	69.3
DG-Net [79]	MT	64.6	83.1	91.5	94.3	CycAs [57]	None	26.7	50.1	-	-
CycAs [57]	None	64.8	84.8	-	-	SPCL [22]	None	19.1	42.3	55.6	61.2
MMT [21]	MT	75.6	89.3	95.8	97.5	SPCL [22]	Ma	26.8	53.7	65.0	69.8
SPCL [22]	None	73.1	88.1	95.1	97.0	MPRD [29]	None	14.6	37.7	51.3	57.1
SPCL [22]	MT	77.5	89.7	96.1	97.6	HCD [71]	None	26.9	53.7	65.3	70.2
MPRD [29]	None	51.1	83.0	91.3	93.6	ICE [3]	None	29.8	59.0	71.7	77.0
ICE [3]	None	79.5	92.0	97.0	98.1	Cluster [9]	None	33.3	63.3	73.7	77.8
HCD [71]	MT	80.2	91.4	-	-	MCL, 50%	None	38.2	66.5	75.2	79.7
Cluster [9]	None	82.6	93.0	97.0	98.1						
MCL, 50%	None	82.9	92.7	97.6	98.7						

Visualization of Feature Distributions. In Figure 5 (b), we visualize the distributions of the features using t-SNE [50] on MSMT17. We compare the feature distribution with the baseline scheme of *All*, and observe that the features of different identities are better clearly separated for our scheme *MCL, 50%*, which demonstrates our learned ReID representations are more discriminative.

4.6 Comparison with State-of-the-arts

Although this work is the first attempt to achieve the unsupervised ReID learning while considering the computational cost savings, we also compare MCL to the state-of-the-art U-ReID methods that without considering resource limitations. From Table 6, we can see that *MCL, 50%* using only 50% unlabeled data for meta-clustering achieves a comparable U-ReID performance compared to SOTA methods, and even outperforms the second best ClusterContrast [9] by 4.9% in mAP on the large-scale MSMT17. In short, MCL is capable of achieving a good trade-off between U-ReID performance and computational costs.

Influence of Clustering Hyper-parameters. As discussed in implementation, we use DBScan and Jaccard distance [73] for first-phase training to cluster with k nearest neighbors ($k=30$) following [9, 22]. For DBScan, the maximum distance d between two samples is set as 0.4 for market1501, 0.7 for other datasets, and the minimal number of neighbors in a core point (denoted as n) is

all set as 4. Here we analyze the influence of these parameters in Figure 7, and conclude that the proposed large-scale unsupervised ReID training method of MCL is robust and stable enough to achieve relatively satisfactory performance with variant hyper-parameters.

5 CONCLUSION

In this paper, we take the first attempt to explore a resource-friendly purely unsupervised person ReID framework, which effectively learns discriminative representations while considering the computational costs. A new concept of meta clustering learning (MCL) is introduced to perform clustering-based ReID training on *partial* unlabeled data, saving the required computing resources. For *the rest data*, we leverage the learned prototypes obtained before as proxy annotator to pseudo-label them. Based on the generated soft pseudo labels, we then polish model with two well-designed losses that take intra- and inter-identity constraints into account for alleviating noisy labels. MCL achieves a SOTA performance on unsupervised ReID, and could also flexibly meet the computing budgets in practice.

6 ACKNOWLEDGEMENTS

This work was supported in part by NSFC under Grant U1908209, 62021001, the National Key Research and Development Program

of China 2018AAA0101400, and NUS Faculty Research Committee Grant (WBS:A-0009440-00-00).

Supplementary

1 LIMITATIONS OF META CLUSTER LEARNING

MCL Cannot Work Well with Too Small Meta-training Data \mathbb{X}_1 . As we described in the manuscript, MCL costs less computing resources in clustering by only using a meta-training subset \mathbb{X}_1 in the first phase for training. Intuitively, if such meta-training subset \mathbb{X}_1 is too small, MCL will be seriously affected by the noisy pseudo label issue so that causes an unsatisfactory U-ReID performance. Taking an extreme case as example for illustration, given a person dataset with 10 IDs and 100 person images, if we split it into 10 subsets and just pick up one as \mathbb{X}_1 , the worst case is that \mathbb{X}_1 may only cover a single person, which will directly make the reference-based pseudo labeling and U-ReID failed. The similar phenomenon also can be observed from Table 7, MCL can not work so well with too small meta-training data \mathbb{X}_1 especially on small-scale datasets, like 20%, on *PersonX* (marked as blue).

The Relationship between Dataset Size and Optimal Split Number Is Not Clear. As we claimed in the manuscript, the larger size of unlabeled dataset, the more superior of the proposed MCL. However, it is difficult to give a deterministic relationship between dataset size and split number. As shown in Table 7, the scheme of *All* that directly conduct clustering over full data achieves the best ReID performance on *PersonX* and *Market1501*, the scheme of *MCL, 50%* achieves the best ReID performance on *MSMT17*, and the scheme of *MCL, 33%* achieves the best ReID performance on the largest *LaST*. We conclude that the larger size of unlabeled dataset, MCL might could use more less meta-training data \mathbb{X}_1 (*i.e.*, a big split number) for training to get a satisfactory performance. But, such the relationship that related to the dataset size vs. the optimal number of subsets is not clear now. The exploration about this relationship is also limited by the existing/released public person ReID datasets, or said, not so many large-scale person ReID datasets, so this will be left as our future work.

2 MEET THE COMPUTING BUDGETS IN PRACTICE

Uniquely, our MCL could enable U-ReID to operate at varying computation budgets. As we pointed before, as a by-product of MCL, our trained model could fully leverage the entire unlabeled data set with only a *partial* subset doing clustering. Such *ratio* can be flexibly determined according to the practical computing power. Given a computing budget, we compare the U-ReID performance of MCL with the *Naive Splitting Training* scheme (*i.e.*, *sequentially* using subsets to meet resource requirements). As the two curves shown in Figure 6, MCL consistently outperforms *Naive Splitting Training* on the two largest datasets *MSMT17* and *LaST*. That is, given a limited budget, MCL could achieve a better discriminative ReID representation learning.

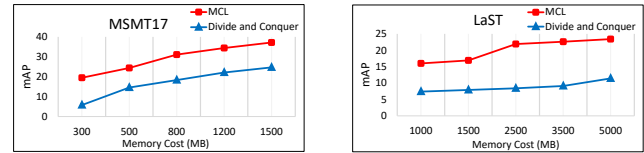


Figure 6: Given a limited memory budget, MCL could achieve a better discriminative representations learning, outperforming *Naive Splitting Training* scheme on the variable budgets.

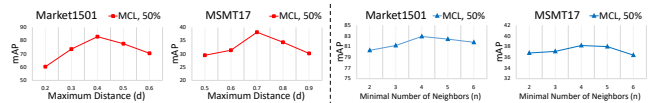


Figure 7: Hyper-parameters exploration for the clustering algorithm of DBScan, where we conduct experiments on *Market1501* and *MSMT17* with the scheme of *MCL, 50%*.

3 HYPER-PARAMETER ANALYSIS

Influence of the Loss Balance. As we described in the manuscript, we design a siamese consistency loss \mathcal{L}_{sc} and a soft-weighted triplet loss \mathcal{L}_{tri}^{sw} in the second polishment phase of meta-clustering learning (MCL) to alleviate the noisy pseudo label issue, which process can be formulated by $\mathcal{L}_{phase2} = \mathcal{L}_{sc} + \lambda * \mathcal{L}_{tri}^{sw}$, the hyper-parameter λ is used to balance the importance between the siamese consistency loss \mathcal{L}_{sc} and the soft-weighted triplet loss \mathcal{L}_{tri}^{sw} . For λ , we initially set it to 1.0, and then coarsely determine it based on the corresponding loss values and its gradients observed during the training. The decision principle is to set its value to make the loss value/gradient lie in a similar range. Grid search within a small range of the derived λ is further employed to get better parameter. Actually, we observed the final performance is not very sensitive to this hyper-parameter, we experimentally set $\lambda = 1.0$ in the end.

4 SOCIAL IMPACT

Positive. In this paper, we introduce the Meta Clustering Learning (termed as MCL), a new concept for large-scale person re-identification. To our best knowledge, this paper is the first attempt to develop an efficient unsupervised person ReID training framework to fully leverage the numerous pedestrian surveillance data while taking the computational cost into account. This is very important for both of academic community and industry, and is also valuable and meaningful to bridge the gap between the fast-developing ReID algorithms and practical applications.

This paper also has the potential to provide new insights to the person ReID field and accelerate the development of ReID algorithms. We improve ReID model's learning ability, enabling the models to be trained with limited computing resources in practical applications. Moreover, the prototype-referenced pseudo labeling idea, and the well-designed intra- and inter-identity constraints are conceptually suitable for a wide range of tasks: from person detection, matching, retrieval to fine-grained person tracking, *etc.*

Negative. Due to the urgent demand of public safety and increasing number of surveillance cameras, person ReID is imperative in intelligent surveillance systems with significant research impact and

Table 7: Memory&Time Cost vs. Unsupervised ReID Performance (%). In which, $M(MB)$, $T(s)$ denotes the *memory cost*, *time cost* of performing clustering once in training, where ‘s’ means ‘second’. $T(h)$ denotes the total training time where ‘h’ means ‘hour’. We compare several MCL variants to baseline (*All*) by using 50%, 33%, 25%, and 20% data randomly selected from the entire unlabeled dataset as meta-training subset \mathbb{X}_1 . For the smallest dataset PersonX [47], it is not necessary to do experiments with too harsh computational requirements (e.g., 33%, 25%, 20%). We can see that the larger size of unlabeled dataset, the more superior of our method (red). Note that, the DukeMTMC-ReID dataset [42] has been taken down and thus not used in our experiment, we just use PersonX [47], Market1501 [70], MSMT17 [58], and LaST [45] for experiments.

Methods	PersonX (9.8k imgs, 410 IDs)					Market1501 (12.9k imgs, 751 IDs)					MSMT17 (32.6k imgs, 1041 IDs)					LaST (71.2k imgs, 5000 IDs)				
	mAP	Rank1	M (MB)	T (s)	T (h)	mAP	Rank1	M (MB)	T (s)	T (h)	mAP	Rank1	M (MB)	T (s)	T (h)	mAP	Rank1	M (MB)	T (s)	T (h)
All	88.5	95.8	822.3	30.0	2.7	83.3	93.0	876.3	34.3	2.9	33.4	62.9	6251.5	118.3	9.3	19.8	74.0	22398.5	494.8	42.0
50%	79.0	93.5	412.6	13.1	2.2	82.9	92.7	348.6	10.8	2.4	38.2	66.5	1761.3	31.1	4.6	20.0	74.9	5779.6	121.2	20.0
33%	–	–	–	–	–	79.6	91.9	287.5	7.0	2.2	31.5	57.4	889.1	18.2	3.8	22.7	75.0	2688.2	70.8	14.0
25%	–	–	–	–	–	75.4	89.3	235.1	5.4	2.0	25.9	53.4	556.9	13.4	3.0	17.2	69.0	1564.2	44.7	9.0
20%	–	–	–	–	–	41.3	61.3	141.4	4.6	1.9	20.1	47.4	394.6	10.3	2.6	15.8	56.0	1066.0	38.4	7.0

practical importance, but this task also might raise questions about the risk of leaking private information. On the other hand, the data collected from the surveillance equipments or downloaded from the internet may violate the privacy of human beings. Therefore, we appeal and encourage further person ReID work to understand and avoid as much as possible the risks of using these pedestrian data. We also encourage research that understands and mitigates the risks arising from surveillance applications. A short-term solution may be developing detection systems. Besides, we recommend researchers to stop the spread of private datasets.

REFERENCES

- [1] Yan Bai, Jile Jiao, Wang Ce, Jun Liu, Yihang Lou, Xuetao Feng, and Ling-Yu Duan. 2021. Person30k: A dual-meta generalization network for person re-identification. In *CVPR*. 2123–2132.
- [2] Mathilde Caron, Ishan Misra, Julien Mairal, Priya Goyal, Piotr Bojanowski, and Armand Joulin. 2020. Unsupervised learning of visual features by contrasting cluster assignments. *NeurIPS* (2020).
- [3] Hao Chen, Benoit Lagadec, and Francois Bremond. 2021. ICE: Inter-instance Contrastive Encoding for Unsupervised Person Re-identification. *ICCV* (2021).
- [4] Ting Chen, Simon Kornblith, Mohammad Norouzi, and Geoffrey Hinton. 2020. A simple framework for contrastive learning of visual representations. In *ICML*. PMLR, 1597–1607.
- [5] Ting Chen, Simon Kornblith, Kevin Swersky, Mohammad Norouzi, and Geoffrey Hinton. 2020. Big self-supervised models are strong semi-supervised learners. *arXiv preprint arXiv:2006.10029* (2020).
- [6] Xinlei Chen, Haoqi Fan, Ross Girshick, and Kaiming He. 2020. Improved baselines with momentum contrastive learning. *arXiv preprint arXiv:2003.04297* (2020).
- [7] Xinlei Chen and Kaiming He. 2021. Exploring simple siamese representation learning. In *CVPR*. 15750–15758.
- [8] Yongxing Dai, Yifan Sun, Jun Liu, Zekun Tong, Yi Yang, and Ling-Yu Duan. 2022. Bridging the Source-to-target Gap for Cross-domain Person Re-Identification with Intermediate Domains. *arXiv preprint arXiv:2203.01682* (2022).
- [9] Zuozhuo Dai, Guangyuan Wang, Weihao Yuan, Siyu Zhu, and Ping Tan. 2021. Cluster Contrast for Unsupervised Person Re-Identification. *arXiv preprint arXiv:2103.11568* (2021).
- [10] Jia Deng, Wei Dong, Richard Socher, Li-Jia Li, Kai Li, and Li-Fei-Fei. 2009. Imagenet: A large-scale hierarchical image database. In *CVPR*.
- [11] Weijian Deng, Liang Zheng, Qixiang Ye, Guoliang Kang, Yi Yang, and Jianbin Jiao. 2018. Image-image domain adaptation with preserved self-similarity and domain-dissimilarity for person re-identification. In *CVPR*.
- [12] Yuhang Ding, Hehe Fan, Mingliang Xu, and Yi Yang. 2020. Adaptive exploration for unsupervised person re-identification. *ACM Transactions on Multimedia Computing, Communications, and Applications (TOMM)* 16, 1 (2020), 1–19.
- [13] Martin Ester, Hans-Peter Kriegel, Jörg Sander, Xiaowei Xu, et al. 1996. A density-based algorithm for discovering clusters in large spatial databases with noise.. In *Kdd*, Vol. 96. 226–231.
- [14] Hehe Fan, Liang Zheng, Chenggang Yan, and Yi Yang. 2018. Unsupervised person re-identification: Clustering and fine-tuning. *ACM Transactions on Multimedia Computing, Communications, and Applications (TOMM)* (2018).
- [15] Ruoyu Feng, Xin Jin, Zongyu Guo, Runsen Feng, Yixin Gao, Tianyu He, Zhizheng Zhang, Simeng Sun, and Zhibo Chen. 2022. Image Coding for Machines with Omnipotent Feature Learning. *ECCV* (2022).
- [16] Dengpan Fu, Dongdong Chen, Jianmin Bao, Hao Yang, Lu Yuan, Lei Zhang, Houqiang Li, and Dong Chen. 2021. Unsupervised Pre-training for Person Re-identification. In *CVPR*. 14750–14759.
- [17] Dengpan Fu, Dongdong Chen, Hao Yang, Jianmin Bao, Lu Yuan, Lei Zhang, Houqiang Li, Fang Wen, and Dong Chen. 2022. Large-Scale Pre-training for Person Re-identification with Noisy Labels. *CVPR* (2022).
- [18] Yang Fu, Yunchao Wei, Guanshuo Wang, Xi Zhou, Honghui Shi, and Thomas S. Huang. 2019. Self-similarity Grouping: A Simple Unsupervised Cross Domain Adaptation Approach for Person Re-identification. *ICCV* (2019).
- [19] Yang Fu, Yunchao Wei, Yuqian Zhou, et al. 2019. Horizontal pyramid matching for person re-identification. In *AAAI*.
- [20] Wenheng Ge, Chunyan Pan, Ancong Wu, Hongwei Zheng, and Wei-Shi Zheng. 2021. Cross-Camera Feature Prediction for Intra-Camera Supervised Person Re-identification across Distant Scenes. In *ACMMM*. 3644–3653.
- [21] Yixiao Ge, Dapeng Chen, and Hongsheng Li. 2020. Mutual mean-teaching: Pseudo label refinery for unsupervised domain adaptation on person re-identification. *ICLR* (2020).
- [22] Yixiao Ge, Feng Zhu, Dapeng Chen, Rui Zhao, and Hongsheng Li. 2020. Self-paced contrastive learning with hybrid memory for domain adaptive object re-id. *NeurIPS* (2020).
- [23] Jean-Bastien Grill, Florian Strub, Florent Altché, Corentin Tallec, Pierre H. Richemond, Elena Buchatskaya, Carl Doersch, Bernardo Avila Pires, Zhaohan Daniel Guo, Mohammad Gheshlaghi Azar, et al. 2020. Bootstrap your own latent: A new approach to self-supervised learning. *arXiv preprint arXiv:2006.07733* (2020).
- [24] Kaiming He, Haoqi Fan, Yuxin Wu, Saining Xie, and Ross Girshick. 2020. Momentum contrast for unsupervised visual representation learning. In *CVPR*. 9729–9738.
- [25] Kaiming He, Xiangyu Zhang, Shaoqing Ren, et al. 2016. Deep residual learning for image recognition. In *CVPR*.
- [26] Lingxiao He, Wu Liu, Jian Liang, Kecheng Zheng, Xingyu Liao, Peng Cheng, and Tao Mei. 2021. Semi-Supervised Domain Generalizable Person Re-Identification. *arXiv preprint arXiv:2108.05045* (2021).
- [27] Alexander Hermans, Lucas Beyer, and Bastian Leibe. 2017. In defense of the triplet loss for person re-identification. *arXiv preprint arXiv:1703.07737* (2017).
- [28] Takashi Isoke, Dong Li, Lu Tian, Weihua Chen, Yi Shan, and Shengjin Wang. 2021. Towards Discriminative Representation Learning for Unsupervised Person Re-identification. *ICCV* (2021).
- [29] Haoxuanye Ji, Le Wang, Sanping Zhou, Wei Tang, Nanning Zheng, and Gang Hua. 2021. Meta Pairwise Relationship Distillation for Unsupervised Person Re-Identification. In *ICCV*. 3661–3670.
- [30] Xin Jin, Cuiling Lan, Wenjun Zeng, and Zhibo Chen. 2020. Global distance-distributions separation for unsupervised person re-identification. In *ECCV*. Springer, 735–751.
- [31] Xin Jin, Cuiling Lan, Wenjun Zeng, Zhibo Chen, and Li Zhang. 2020. Style Normalization and Restitution for Generalizable Person Re-identification. In *CVPR*.
- [32] Ron Kohavi et al. 1995. A study of cross-validation and bootstrap for accuracy estimation and model selection. In *Ijcai*, Vol. 14. Montreal, Canada, 1137–1145.

- [33] Minxian Li, Xiatian Zhu, and Shaogang Gong. 2018. Unsupervised person re-identification by deep learning tracklet association. In *ECCV*.
- [34] Minxian Li, Xiatian Zhu, and Shaogang Gong. 2019. Unsupervised Tracklet Person Re-Identification. *TPAMI* (2019).
- [35] Shan Lin, Haoliang Li, Chang-Tsun Li, and Alex Chichung Kot. 2018. Multi-task mid-level feature alignment network for unsupervised cross-dataset person re-identification. *BMVC* (2018).
- [36] Yutian Lin, Xuanyi Dong, Liang Zheng, Yan Yan, and Yi Yang. 2019. A bottom-up clustering approach to unsupervised person re-identification. In *AAAI*, Vol. 33. 8738–8745.
- [37] Yutian Lin, Lingxi Xie, Yu Wu, Chenggang Yan, and Qi Tian. 2020. Unsupervised person re-identification via softened similarity learning. In *CVPR*. 3390–3399.
- [38] Jiawei Liu, Zheng-Jun Zha, Di Chen, Richang Hong, and Meng Wang. 2019. Adaptive Transfer Network for Cross-Domain Person Re-Identification. In *CVPR*.
- [39] Aaron van den Oord, Yazhe Li, and Oriol Vinyals. 2018. Representation learning with contrastive predictive coding. *arXiv preprint arXiv:1807.03748* (2018).
- [40] Lei Qi, Lei Wang, Jing Huo, Luping Zhou, Yinghuan Shi, and Yang Gao. 2019. A Novel Unsupervised Camera-aware Domain Adaptation Framework for Person Re-identification. *ICCV* (2019).
- [41] Sucheng Ren, Daquan Zhou, Shengfeng He, Jiashi Feng, and Xinchao Wang. 2022. Shunted Self-Attention via Multi-Scale Token Aggregation. In *CVPR*. 10853–10862.
- [42] Ergys Ristani, Francesco Solera, Roger Zou, Rita Cucchiara, and Carlo Tomasi. 2016. Performance measures and a data set for multi-target, multi-camera tracking. In *ECCV*.
- [43] Youngmin Ro, Jongwon Choi, Dae Ung Jo, Byeongho Heo, Jongin Lim, and Jin Young Choi. 2019. Backbone cannot be trained at once: Rolling back to pre-trained network for person re-identification. In *AAAI*, Vol. 33. 8859–8867.
- [44] Florian Schroff, Dmitry Kalenichenko, and James Philbin. 2015. Facenet: A unified embedding for face recognition and clustering. In *CVPR*.
- [45] Xiujun Shu, Xiao Wang, Shiliang Zhang, Xianghao Zhang, Yuanqi Chen, Ge Li, and Qi Tian. 2021. Large-Scale Spatio-Temporal Person Re-identification: Algorithm and Benchmark. *arXiv preprint arXiv:2105.15076* (2021).
- [46] Liangchen Song, Cheng Wang, Lefei Zhang, Bo Du, Qian Zhang, Chang Huang, and Xinggang Wang. 2020. Unsupervised domain adaptive re-identification: Theory and practice. *Pattern Recognition* (2020), 107173.
- [47] Xiaoxiao Sun and Liang Zheng. 2019. Dissecting person re-identification from the viewpoint of viewpoint. In *CVPR*. 608–617.
- [48] Yifan Sun, Liang Zheng, Yi Yang, Qi Tian, and Shengjin Wang. 2018. Beyond part models: Person retrieval with refined part pooling (and a strong convolutional baseline). In *ECCV*. 480–496.
- [49] Haotian Tang, Yiru Zhao, and Hongtao Lu. 2019. Unsupervised Person Re-Identification With Iterative Self-Supervised Domain Adaptation. In *CVPR workshops*.
- [50] Laurens Van der Maaten and Geoffrey Hinton. 2008. Visualizing data using t-SNE. *Journal of machine learning research* 9, 11 (2008).
- [51] Joaquin Vanschoren. 2018. Meta-learning: A survey. *arXiv preprint arXiv:1810.03548* (2018).
- [52] Joaquin Vanschoren. 2019. Meta-learning. In *Automated Machine Learning*. Springer, Cham, 35–61.
- [53] Ricardo Vilalta and Youssef Drissi. 2002. A perspective view and survey of meta-learning. *Artificial intelligence review* 18, 2 (2002), 77–95.
- [54] Dongkai Wang and Shiliang Zhang. 2020. Unsupervised person re-identification via multi-label classification. In *CVPR*. 10981–10990.
- [55] Jingya Wang, Xiatian Zhu, Shaogang Gong, and Wei Li. 2018. Transferable joint attribute-identity deep learning for unsupervised person re-identification. In *CVPR*.
- [56] Yanan Wang, Shengcai Liao, and Ling Shao. 2020. Surpassing real-world source training data: Random 3d characters for generalizable person re-identification. In *ACMMM*. 3422–3430.
- [57] Zhongdao Wang, Jingwei Zhang, Liang Zheng, Yixuan Liu, Yifan Sun, Yali Li, and Shengjin Wang. 2020. CycAs: Self-supervised Cycle Association for Learning Re-identifiable Descriptions. In *ECCV*. Springer, 72–88.
- [58] Longhui Wei, Shiliang Zhang, Wen Gao, and Qi Tian. 2018. Person transfer GAN to bridge domain gap for person re-identification. In *CVPR*.
- [59] Jinlin Wu, Yang Yang, Hao Liu, Shengcai Liao, Zhen Lei, and Stan Z Li. 2019. Unsupervised graph association for person re-identification. In *ICCV*. 8321–8330.
- [60] Yiming Wu, Xintian Wu, Xi Li, and Jian Tian. 2021. MGH: Metadata Guided Hypergraph Modeling for Unsupervised Person Re-identification. In *ACMMM*. 1571–1580.
- [61] Zhirong Wu, Yuanjun Xiong, Stella X Yu, and Dahua Lin. 2018. Unsupervised feature learning via non-parametric instance discrimination. In *CVPR*. 3733–3742.
- [62] Fengxiang Yang, Ke Li, Zhun Zhong, Zhiming Luo, Xing Sun, Hao Cheng, Xiaowei Guo, Feiyue Huang, Rongrong Ji, and Shaozi Li. 2020. Asymmetric Co-Teaching for Unsupervised Cross Domain Person Re-Identification. *AAAI* (2020).
- [63] Qize Yang, Hong-Xing Yu, Ancong Wu, and Wei-Shi Zheng. 2019. Patch-Based Discriminative Feature Learning for Unsupervised Person Re-Identification. In *CVPR*.
- [64] Zizheng Yang, Xin Jin, Kecheng Zheng, and Feng Zhao. 2022. Unleashing the Potential of Unsupervised Pre-Training with Intra-Identity Regularization for Person Re-Identification. *CVPR* (2022).
- [65] Hong-Xing Yu, Wei-Shi Zheng, Ancong Wu, Xiaowei Guo, Shaogang Gong, and Jian-Huang Lai. 2019. Unsupervised Person Re-identification by Soft Multilabel Learning. In *CVPR*.
- [66] Kaiwei Zeng, Munan Ning, Yaohua Wang, and Yang Guo. 2020. Hierarchical clustering with hard-batch triplet loss for person re-identification. In *CVPR*. 13657–13665.
- [67] Yunpeng Zhai, Shijian Lu, Qixiang Ye, Xuebo Shan, Jie Chen, Rongrong Ji, and Yonghong Tian. 2020. AD-Cluster: Augmented discriminative clustering for domain adaptive person re-identification. In *CVPR*. 9021–9030.
- [68] Xinyu Zhang, Jiawei Cao, Chunhua Shen, and Mingyu You. 2019. Self-training with progressive augmentation for unsupervised cross-domain person re-identification. In *ICCV*.
- [69] Xinyu Zhang, Dongdong Li, Zhigang Wang, Jian Wang, Errui Ding, Javen Qinfeng Shi, Zhaoxiang Zhang, and Jingdong Wang. 2022. Implicit Sample Extension for Unsupervised Person Re-Identification. In *CVPR*. 7369–7378.
- [70] Liang Zheng, Liyue Shen, et al. 2015. Scalable person re-identification: A benchmark. In *ICCV*.
- [71] Yi Zheng, Shixiang Tang, Guolong Teng, Yixiao Ge, Kaijian Liu, Jing Qin, Donglian Qi, and Dapeng Chen. 2021. Online Pseudo Label Generation by Hierarchical Cluster Dynamics for Adaptive Person Re-Identification. In *ICCV*. 8371–8381.
- [72] Yi Zheng, Yong Zhou, Jiaqi Zhao, Ying Chen, Rui Yao, Bing Liu, and Abdulmotaleb El Saddik. 2022. Clustering Matters: Sphere Feature for Fully Unsupervised Person Re-identification. *ACM Transactions on Multimedia Computing, Communications, and Applications (TOMM)* 18, 4 (2022), 1–18.
- [73] Zhun Zhong, Liang Zheng, Donglin Cao, and Shaozi Li. 2017. Re-ranking person re-identification with k-reciprocal encoding. In *CVPR*.
- [74] Zhun Zhong, Liang Zheng, Guoliang Kang, Shaozi Li, and Yi Yang. 2020. Random erasing data augmentation. In *Proceedings of the AAAI Conference on Artificial Intelligence*, Vol. 34. 13001–13008.
- [75] Zhun Zhong, Liang Zheng, Shaozi Li, and Yi Yang. 2018. Generalizing a person retrieval model hetero-and homogeneously. In *ECCV*.
- [76] Zhun Zhong, Liang Zheng, Zhiming Luo, Shaozi Li, and Yi Yang. 2019. Invariance matters: Exemplar memory for domain adaptive person re-identification. In *CVPR*. 598–607.
- [77] Jun-Yan Zhu, Taesung Park, Phillip Isola, et al. 2017. Unpaired image-to-image translation using cycle-consistent adversarial networks. In *ICCV*.
- [78] Weiming Zhuang, Yonggang Wen, and Shuai Zhang. 2021. Joint optimization in edge-cloud continuum for federated unsupervised person re-identification. In *ACMMM*. 433–441.
- [79] Yang Zou, Xiaodong Yang, Zhiding Yu, BVK Vijaya Kumar, and Jan Kautz. 2020. Joint disentangling and adaptation for cross-domain person re-identification. In *ECCV*. Springer, 87–104.